Available online at www.sciencedirect.com
SCIENCE DIRECT®
Surface Science 545 (2003) 143–153
SURFACE SCIENCE
www.elsevier.com/locate/susc

Adsorption and reaction on pristine and oxidized Co–Pd bimetallic particles supported on Al_2O_3 thin films

A.F. Carlsson, M. Naschitzki, M. Bäumer *, H.-J. Freund

Department of Chemical Physics, Fritz-Haber-Institut der Max-Planck-Gesellschaft, Faradayweg 4-6, 14195 Berlin, Germany

Received 2 July 2003; accepted for publication 8 September 2003

Abstract

A model for bimetallic Co–Pd systems known to be active as Fischer–Tropsch catalysts has been constructed and studied under ultra-high vacuum conditions with respect to its adsorption and reaction properties. It was previously shown that subsequent deposition of Pd and Co results in the formation of core-shell structures; the morphology of the bimetallic particles can be controlled taking advantage of the different nucleation and growth behavior of Pd and Co. In this study, the reactive properties of pristine and oxidized bimetallic Co–Pd particles with O_2, CO, D_2, C_2D_4, and C_2H_4 have been investigated using temperature programmed desorption and reaction spectroscopy. Hydrogen and CO adsorption is facile on the non-oxidized particles, but is severely inhibited on the oxidized particles. Ethylene binds to the non-oxidized particles in π-bonded and di-σ-bonded configurations and dehydrogenates to form ethylidyne. In contrast, on the oxidized particles, only the π-bonded species is formed. To slightly different degrees, the bimetallic or monometallic particles are active for ethylene hydrogenation; the oxidized particles are essentially non-active for ethylene hydrogenation.

Keywords: Palladium; Cobalt; Catalysis; Thermal desorption spectroscopy

1. Introduction

Iron and cobalt-based catalysts were originally found in 1926 to produce gasoline from syngas ($CO + H_2$) in what is now termed the Fischer–Tropsch (F–T) process [1]. Although Ni [2] and Ru [3] are also active in the conversion of syngas to hydrocarbons, most catalysts still use Co or Fe [4]. Pichler [5] noted that active F–T catalysts were active for hydrogenation reactions and were capable of metal–carbonyl bond formation. Fe-based F–T catalysts generally have a higher activity towards the water-gas shift reaction than Co, making Fe-based catalysts more suited to process CO-rich syngas produced from coal while Co-based catalysts are more suited to process H_2-rich syngas produced from natural gas. Thus, recent efforts to produce diesel fuel from natural gas have focused on Co-based catalysts [4].

Many detailed reaction mechanisms for the hydrocarbon-chain building F–T reaction have been proposed, and there has been considerable

* Corresponding author. Present address: Institut für Angewandte und Physikalische Chemie, Universität Bremen, Leobener Str. NW2, Postfach 330440, 28334 Bremen, Germany. Tel.: +421-2182500; fax: +421-2184918.

E-mail addresses: mbaeumer@uni-bremen.de, baeumer@fhi-berlin.mpg.de (M. Bäumer).

0039-6028/$ - see front matter © 2003 Elsevier B.V. All rights reserved.
doi:10.1016/j.susc.2003.09.012

debate over them [4,6]. One general mechanistic category suggests that CO units are built into a chain, with the oxygen atom being removed only after the unit is added. This is termed the surface carbonate mechanism, and is thought to operate on Fe catalysts [6]. Another model suggests that CH_2 units are built on the surface before becoming polymerized into a chain, whose end CH_2 unit is fixed to the surface [4]. This second mechanism is a version of the surface-carbide mechanism and is thought to occur on Co catalysts [6].

Notably, the conversion of methane to higher hydrocarbons [7] and hydrogenation of CO [8–10] shows greater reactivity on Co–Pd bimetallic supported catalysts than either metal alone. It has been proposed that the additional Pd facilitates the adsorption of H_2, which spills over and reduces CoO formed during the reaction [7–15].

In order to shed more light on the adsorption and reaction properties of Co–Pd bimetallic particles, we have conducted a corresponding model study under ultra-high vacuum conditions using CO, D_2, C_2D_4, and C_2H_4 as adsorbates.

In this context, it is interesting to note that the adsorption of ethylene may be used to model Fischer–Tropsch intermediates because it forms ethylidyne which is similar to the intermediate proposed for the surface-carbide mechanism of the Fischer–Tropsch reaction. On Pd surfaces [16,17], the adsorption of ethylene results in a π-bonded state at low temperature which then converts to a di-σ bonded state at intermediate temperature. Around room temperature, there is a hydrogen rearrangement and elimination, resulting in a (CH_3–C$\equiv$) species, called ethylidyne, bound to the surface by the triple bond. The eliminated H may then hydrogenate another ethylene molecule—a process called self-hydrogenation—or recombine with another H atom to form H_2, which desorbs. On supported Pd particles, both π-bonded and di-σ bonded ethylene have been detected at 90 K. Also in this case, heating to 300 K resulted in the formation of ethylidyne [18]. At higher temperatures, the ethylidyne decomposes to surface-carbon, resulting in the further desorption of H_2. Ethylidyne is similarly formed on Co surfaces [16].

Apart from the pristine systems, experiments with particles exposed to oxygen have been carried out, in order to investigate the influence of oxide phases formed during the F–T process. Here, it is important to know that CoO is formed immediately at 300 K on close-packed Co(0 0 0 1) [19,20]. On Co(1 0 $-$1 0), ordered structures of adsorbed oxygen are formed at different coverages [21] which lead to surface reconstructions. The interaction of oxygen with Co is strong enough that oxygen either goes sub-surface or reconstructs the surface at low pressures; thus we refer to the oxygen treated Co particles as CoO in the following [22]. In contrast to Co, Pd does not form an oxide as readily [23–27], but does easily form a chemisorbed p(2$\times$2) oxygen overlayer on the (1 1 1) face [26,28]. For this reason, we will refer to the Pd particles as being oxygen-covered.

The preparation and structural properties of the model systems used in this study are well known. The growth and morphology of Pd [29], Co [30] and Co–Pd bimetallic [31] particles deposited on a thin alumina film [32] grown on NiAl(1 1 0) have been characterized previously in detail. STM images show that at 300 K the majority of Pd particles nucleate and grow at antiphase and reflection domain boundaries of the alumina film [29]. Closer inspection of the triangular-shaped Pd particles revealed a crystalline structure with (1 1 1) faces terminating the aggregates [33]. In contrast, pure Co nucleates at point defects of the alumina film under these conditions, as shown by STM [22,34]. Here, no indications of crystalline order were detected. At temperatures above 300 K, where Co atoms on the surface are more mobile, nucleation increasingly occurs at line defects [30]; in general, Co atoms are less mobile than Pd atoms on the alumina substrate due to a stronger metal–substrate interaction [30]. Whereas Pd preferentially nucleates on Co particles previously deposited on the alumina surface [31], evaporated Co metal nucleates at point defects between as well as on top of Pd particles previously deposited on the alumina surface and nucleated at line defects [31], because it is less mobile. Thus, sequential deposition of Co and Pd results in a core-shell structure, where the second metal deposited forms the shell (see sketches in Fig. 1).

In addition to the structural characterization, first TPD results regarding the interaction of CO with the Co–Pd model systems have been pub-

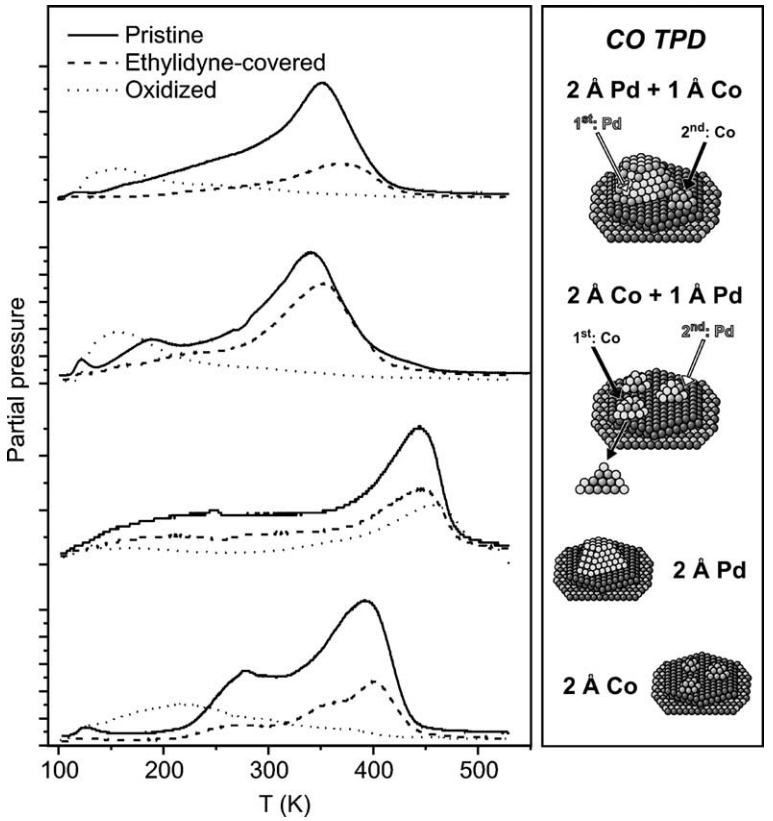

Fig. 1. TPD of CO from the pristine, ethylidyne-covered, and oxygen treated Co–Pd particles.

lished recently [31]. Briefly, the binding energy of CO to both Pd and Co sites is lowered by the presence of the other metal. The preferred CO-adsorption site on each metal is different: atop sites in the case of Co and 3-fold hollow sites in the case of Pd. Co-atop sites are better preserved at various bimetallic compositions because they are statistically less vulnerable than the Pd 3-fold hollow sites. The CO-adsorption study and a brief calculation based on particle shape indicate that 1 Å Co forms an incomplete shell on top of 2 Å Pd when deposited at 300 K and vice versa.

2. Experimental

The experimental apparatus used in this study has been described in detail elsewhere [35]. Briefly, it consists of a commercially built analysis chamber (Omicron) with an AFM/STM stage, as well as XPS and LEED. Coupled to the analysis chamber by a transfer system is a preparation chamber containing Pd and Co metal evaporators, and facilities for sputtering, gas dosing, and TPD measurements. The base pressures in the analysis and preparation chamber are 1×10^{-11} and 1×10^{-10} mbar, respectively. The metal evaporators were calibrated both with a quartz microbalance in a different chamber and the STM in the analysis chamber. The average thickness of the film is herein given in Å, where 1 ML is equivalent to 2.03 Å Co or 2.25 Å Pd. The notation "2 Å Co particles" will be used to denote an ensemble of Co particles forming an average thickness of 2 Å, though each particle has roughly the shape of a hemisphere with an average diameter of 27 Å and an average height of 13 Å [31]. The NiAl(1 1 0) crystal was cleaned by cycles of Ar^+ sputtering, and an Al_2O_3 film was prepared by previously described methods [29,32].

During TPD measurements, the sample—pristine or oxygen treated with 30 L O_2 at 300 K—was exposed to ethylene, deuterium, or CO at 100 K and then placed less than 1 mm away from the differentially pumped cap of the quadrupole mass spectrometer. The sample was heated by radiation from a tungsten filament mounted directly behind it. The temperature ramp was accurately programmed with a controller and power supply from H. Schlichting. Blank TPD measurements from the oxide film without deposited metal particles showed that desorption of small amounts of masses 2, 16, 18, 28, 32, and 44 below 150 K were due to desorption from the heating filament; these signals were at least an order of magnitude smaller than those resulting from desorption from the metal particles. The gases investigated do not adsorb on the pristine alumina film above 90 K. In the figures showing TPD of C_2H_4 with the co-evolution of H_2, we have subtracted the cracking pattern contribution of C_2H_4 to the H_2 signal.

3. Results and discussion

The adsorption of CO on pristine Co–Pd bimetallic particles has been previously studied [31]; the relevant data are reproduced in Fig. 1. On 2 Å Co particles, CO desorbs first from a higher-coverage state at about 277 K (further details will be discussed elsewhere), and then from atop sites at about 393 K. In contrast to Co, CO is most strongly bound to 3-fold hollow sites on Pd, from which it desorbs at about 444 K. On the bimetallic particles, the desorption temperature of CO is lowered to about 352 K when 1 Å Co is covering 2 Å Pd particles, and to about 340 K when 1 Å Pd is covering 2 Å Co particles. In the case of the bimetallic particles, the lower temperature peak is broad and may represent desorption from more than one state.

A pre-exposure of oxygen changes the adsorption behavior of CO on the pristine and bimetallic particles. The TPD spectrum of CO from 2 Å Co particles which had previously been exposed to 30 L O_2 at 300 K shows only a smaller, broad peak around 200 K in contrast to the sharper desorption peak around 390 K for the pristine particles (Fig. 1). The surface of the Co particles appears to be mostly oxidized after this exposure, and the interaction of CO with the CoO layer is weak, as expected for an oxide [36]. Nothing of the original desorption feature from Co-atop sites at 390 K is observed for the oxidized particles.

In contrast, a fully developed oxide layer does not form [23–27] at these temperatures on the 2 Å Pd particles, which are composed of mostly (1 1 1) faces [33]. Rather, a chemisorbed p(2×2)-O overlayer is formed on the Pd(1 1 1) faces [26,28] which does not desorb below 700 K [26]. The desorption of CO from Pd 3-fold sites at 440 K is retained, though it is attenuated on the oxygen-covered Pd particles (Fig. 1). It has been shown that on Pd(1 1 1), pre-existing p(2×2)-oxygen overlayers compress into $(\sqrt{3} \times \sqrt{3})$R30-O islands when CO is co-adsorbed; the additional CO forms separate islands of $(\sqrt{3} \times \sqrt{3})$R30-CO rather than a mixed overlayer. Thus, it is reasonable to expect a reduced carrying capacity for CO on the oxygen-precovered Pd particles.

In the case of the bimetallic particles, CO adsorption is largely blocked by chemisorbed oxygen similarly to the case of the pure Co particles (Fig. 1). A subsequent coverage of 1 Å Pd is not enough to completely cover 2 Å Co particles, as would be expected from a simple geometrical calculation or previous TPD studies [31]. When 1 Å Co is covering 2 Å Pd, the Co shell also appears to be fully oxidized, again resulting in the suppression of CO-adsorption except for a signal at low temperature. It is possible that the desorption of CO around 130 K from the bimetallic particles is from CO bound to Pd-atop sites, which we would expect to be most resistant to oxygen-adsorption. Desorption of CO from Pd 3-fold hollow sites is not observed in the case of the pristine or the oxidized particles due to the strong ensemble effect expected for the bimetallic particles [31].

The interaction of hydrogen with the pure and bimetallic particles is dependent on the bimetallic composition, as demonstrated by TPD (Fig. 2). We have used deuterium in place of hydrogen in order to avoid detecting absorbed or sub-surface hydrogen already present from the background gases. On unoxidized 2 Å Co particles, desorption peaks can be seen at 280 and 340 K. On the open

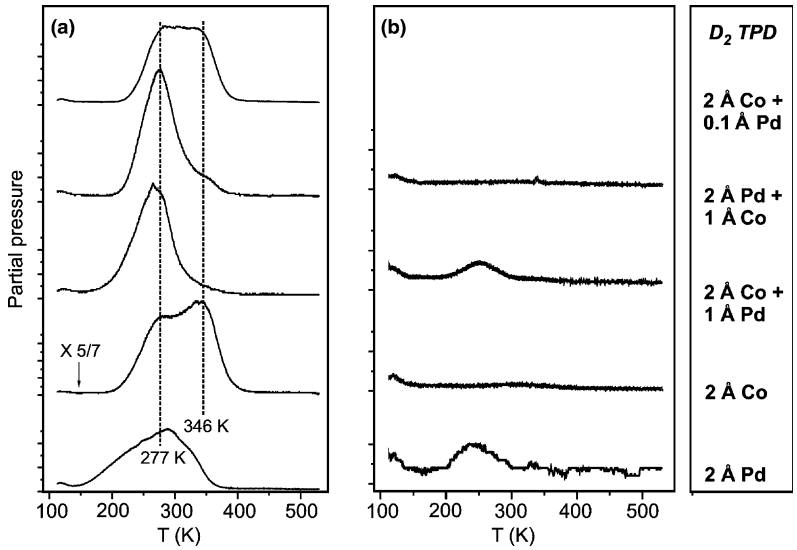

Fig. 2. TPD of D_2 from the pristine (a) and oxygen treated particles (b). All curves in part (b) are on the same partial pressure scale.

Co(10−10) face, hydrogen has been observed to form an ordered c(2×4) overlayer at 0.5 ML, a (2×1)p2 mg overlayer at 1 ML, and cause a reconstruction at a saturation coverage of 1.5 ML [37]. In contrast to Pd, hydrogen does not form a sub-surface species on the open face of Co [37]. The two desorption peaks in Fig. 2a are most likely due to the depopulation of one adsorbate phase after the another, though the structure on the particles is probably not the same as on Co(10−10). On the 2 Å Pd particles, a broader feature can be seen with a peak at 290 K; the desorption before the peak temperature has previously been assigned to sub-surface hydrogen [38]. The interaction of surface-adsorbed hydrogen with Co appears stronger than the interaction with Pd.

The high-temperature desorption feature of hydrogen from Co is affected by the addition of Pd. When 0.1 Å Pd is deposited on top of 2 Å Co particles, the high-temperature desorption peak from the 2 Å Co particles is attenuated (Fig. 2a), indicating that Pd adatoms suppress that adsorption state e.g. by site blocking or prevent the formation of a higher-compression phase. Further, when 1 Å Pd forms a shell on top of 2 Å Co particles, the high-temperature feature present in the desorption spectrum from 2 Å Co particles is almost completely suppressed. When 1 Å Co forms a shell on 2 Å Pd particles, this feature is further seen again, although in this case it may arise from Co particles which have nucleated between existing Pd particles and are thus made of pure Co. The lower-temperature desorption feature of hydrogen from 2 Å Co particles does not appear to be affected by the addition of 0.1 Å Pd or 1 Å Pd, though it is certainly possible that different adsorption states result in similar desorption temperatures.

Sub-surface hydrogen adsorption is also affected by the addition of Co to Pd particles. The lower-temperature tail of hydrogen desorption from pure Pd particles, attributable to sub-surface hydrogen [38], is reduced by the addition of 1 Å Co to 2 Å Pd particles (Fig. 2a). The desorption of surface-bound hydrogen from Pd 3-fold sites also seems to be reduced by the addition of 1 Å Co to 2 Å Pd particles; this could be explained by an ensemble or site-blocking effect. Furthermore, sub-surface hydrogen adsorption appears suppressed when 1 Å Pd is covering 2 Å Co particles. Since pure Co cannot carry sub-surface hydrogen [37], this suggests that the bimetallic Co–Pd particles have less carrying capacity for sub-surface hydrogen than does Pd alone.

The interaction of hydrogen with the pure and bimetallic particles is sensitive to the presence of chemisorbed oxygen, as demonstrated by TPD (Fig. 2b). When the particles were exposed to 30 L of O_2 at 300 K before the D_2 dose and TPD measurement, no D_2 desorption was detected from the 2 Å Co particles or the 2 Å Pd with a 1 Å Co shell on top (Fig. 2b). Only very small amounts of D_2 desorption were detected from the oxygen-covered 2 Å Pd particles (Fig. 2b); apparently, hydrogen can still adsorb, to a limited extent, on the particles having faces with ordered p(2×2)-O overlayers. It is possible that the small amount of hydrogen adsorption occurs at the particle edges or boundary with the substrate, since we would expect a larger amount if it were actually adsorbing within the p(2×2)-O structure. A small amount of D_2 desorption was also detected from 2 Å Co particles covered with 1 Å Pd at the same temperature as the desorption from the pure 2 Å Pd particles. It is possible that this is also due to adsorption of hydrogen on edges of the Pd. In contrast, no D_2 desorption from 2 Å Co was detected, as we might expect from the fully oxidized Co particles. However, it is slightly more surprising that only 1 Å Co added to 2 Å Pd particles also results in a complete suppression of D_2 adsorption when oxidized. Since Co nucleates not only on top of existing Pd particles, but also between them, the Pd particles are not fully covered with Co. Thus, an incomplete layer of Co adatoms on top of Pd particles is sufficient to completely suppress adsorption of D_2. The consequences of the two experiments with bimetallic particles for the Fischer–Tropsch reaction is that Pd added to the Co-catalyst would have to be well exposed to the surface in order to trap hydrogen and thereby facilitate reduction of CoO [7–15]. In none of the cases was the evolution of deuterated water, a possible reaction product, detected.

The adsorption of ethylene on the bimetallic particles is not as drastically affected by previous oxidative treatment as the adsorption of CO or H_2. The desorption of ethylene from 2 Å Pd particles results in a broad desorption feature (Fig. 3a), which has previously been assigned to π-bonded ($T < 230$ K) and di-σ bonded ($T \sim 270$ K) ethylene [38]. It is possible that the broadness of the peak results from these two binding modes at different binding sites on the particles. At 300 K there is desorption of H_2 when ethylidyne is formed from the di-σ boned ethylene [38] on the Pd particles. Further H_2 desorption is due to the stepwise decomposition of ethylidyne to surface carbon. The desorption of ethylene from Co particles is similar to the desorption from Pd particles in that there are a number of desorption states which are followed by a liberation of H_2 (Fig. 3a). The liberation of H_2 near 300 K is most likely due to the formation of ethylidyne and subsequent decomposition, the latter step occurring more readily on Co particles than on Pd particles (Fig. 3a). When 1 Å Pd is covering 2 Å Co particles or vice versa, there is also a desorption of ethylene from π-bonded and di-σ states, as well as the evolution of hydrogen at 300 K. However, the evolution of hydrogen, indicative of the formation of ethylidyne, occurs at 277 K on the bimetallic particles, rather than at 300 K, as on the pure Pd particles or at 293 K as on the pure Co particles. This small but clear difference indicates a facilitation in the reaction of ethylene conversion to ethylidyne on these non-oxidized bimetallic particles. This suggests that the enhancement in F–T reactivity of Co catalysts with added Pd may also be due to properties other than CoO reduction.

On oxygen-covered Pd particles, the amount of π-bonded ethylene remains the same as that on the non-oxidized particles, while the relative amount di-σ bonded ethylene is reduced (Fig. 3b and c). This is probably due to the site-blocking effect of oxygen in Pd 3-fold sites [26,28]. There is a small shoulder due to ethylene desorption around 270 K (Fig. 3b) on the Pd particles suggesting that an oxygen-overlayer on Pd particles hinders the formation of di-σ bonded ethylene but does not fully suppress it. The desorption of ethylene at 270 K followed by evolution of hydrogen at 300 K is further reduced when the surface has been exposed to D_2 before being exposed to C_2H_4 (Fig. 3c). This might be the result of a site blocking effect or due to the fact that part of the ethylene is hydrogenated at lower temperature and thus not available for ethylidyne formation.

On the oxidized Co particles and bimetallic Co–Pd particles, the amount of adsorption into

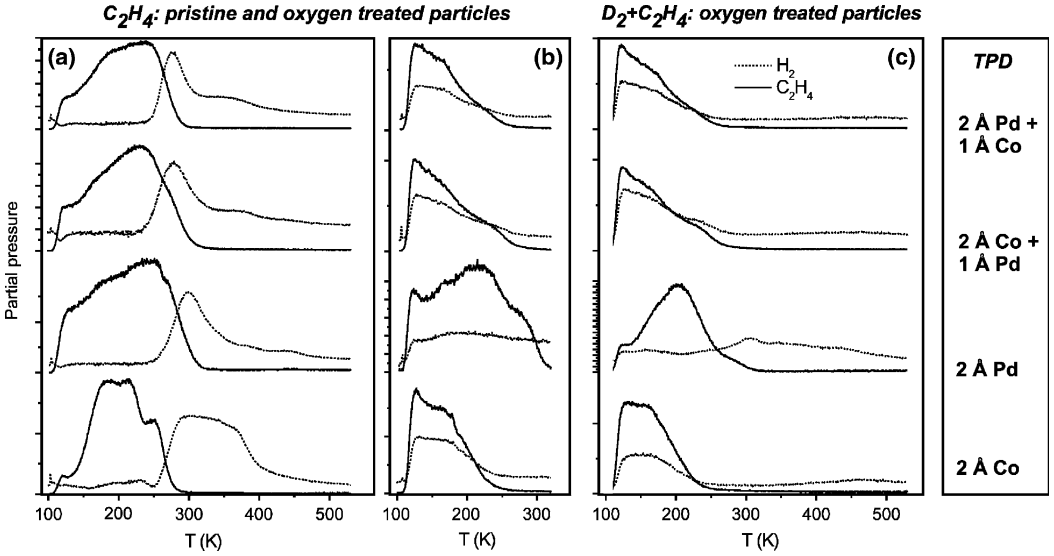

Fig. 3. TPD of C_2H_4 from the pristine (a) and oxygen treated particles (b, c) resulting in the evolution of both C_2H_4 and H_2 from the surface. The spectra shown in part (c) have been obtained after dosing D_2, before C_2H_4 exposure. The H_2 signal has been corrected for the cracking contribution of C_2H_4 in all cases, and is plotted on a different scale. In case of the spectra in part (b), the surface was only heated to 320 K, because the attempt at forming ethylidyne was used for a subsequent experiment. Desorption of H_2O (b) or D_2, H_2O, or D_2O (c) was not observed.

the π-bonded state is roughly the same as on the non-oxidized particles, but the formation of di-σ bonded ethylene is fully suppressed. A pre-dose of D_2 before the ethylene TPD on the oxidized Co and Co–Pd bimetallic particles (Fig. 3c) makes no difference to the ethylene desorption spectrum, because the D_2 cannot adsorb on these particles (Fig. 2b), excepting Pd-covered Co; in the latter case, however, the amount of D_2 adsorption was shown to be low.

An attempt was made at reducing the oxidized particles through a TPD of ethylene up to 320 K. However, the second TPD spectrum of ethylene from the oxidized particles is similar to the first (data not shown). This suggests that CoO cannot be reduced by π-bonded olefins such as ethylene.

TPD of CO after a pre-dose of ethylene and anneal to 320 K shows an attenuated and shifted signal compared with the clean particles (Fig. 1). The attenuation of the CO-desorption feature in the pure and bimetallic particles suggests ethylidyne has formed and is taking up space on the surface. Further, the CO-desorption feature is slightly shifted to higher binding energy, particularly on the bimetallic particles, possibly being the result of a favorable adsorbate–adsorbate interaction.

The hydrogenation of ethylene with pre-adsorbed D_2 was observed on the Co, Pd, and bimetallic particles. Subtracting the background of CO ($\sim 3\times10^{-10}$ mbar) from the parent ion of ethylene suggests that roughly 10% of the ethylene was hydrogenated during the TPD measurement in all cases. Fig. 4a shows the integrated mass to charge ratio detected during the TPD normalized to the overall signal from $m/z = 27$. To be sure, comparing these amounts is complex due to the isomers they represent and also the overlapping cracking patterns. Thus we intend for the data in Fig. 4 only to show the general trends during hydrogenation on the different particle compositions. Lower masses than $m/z = 32$, which would suggest the exchange of one or two hydrogen atoms with deuterium or hydrogenation by hydrogen are the most pronounced. In the latter case, the hydrogen can come either from the C_2H_4 molecule (self-hydrogenation) or from adsorption of H_2 from the background. Mass 32 represents $C_2H_4D_2$, where

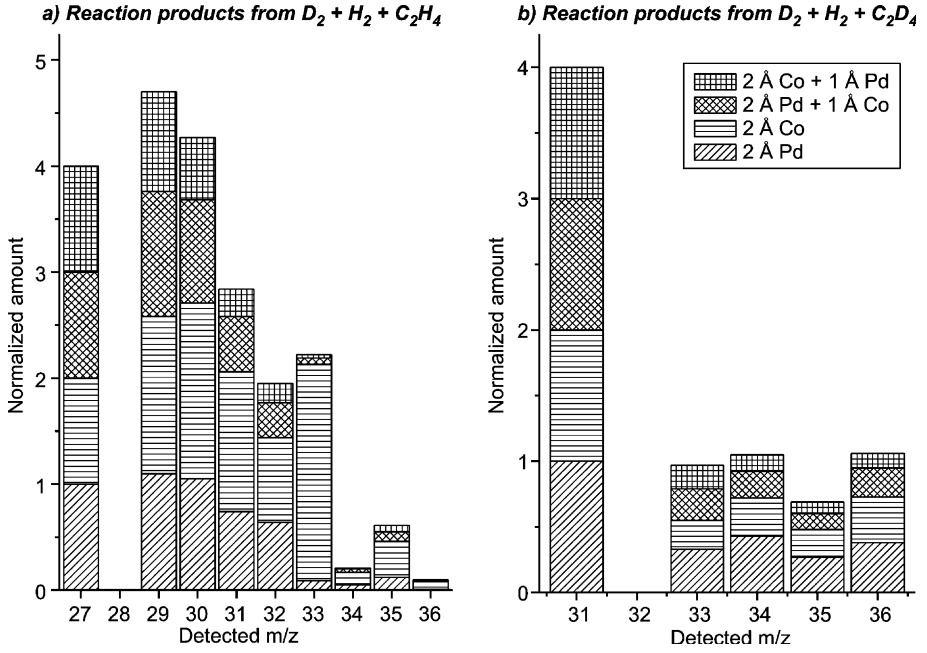

Fig. 4. Relative detected mass to charge ratios resulting from the reaction of D_2 with C_2H_4 and C_2D_4, respectively, on the bimetallic particles. The data were obtained in a multi-mass TPD experiment carried out in the temperature range from 100 to 500 K. In all cases, some H_2 was present in the background.

the existing ethylene has been fully hydrogenated by pre-existing deuterium on the surface. Interestingly, the Co particles seem to be good for hydrogenation alone, and the Co–Pd bimetallic combinations do not appear significantly better or worse than the clean metals. There are significant amounts of masses 33 through 36, indicating not only the addition of deuterium, but also an exchange of surface deuterium with hydrogen from the original C_2H_4 molecule before subsequent addition of deuterium to form ethane. In particular, pure Co appears effective at exchanging a hydrogen atom for a deuterium before adding two more deuterium atoms to form mass 33. An analogy can be drawn with a previously proposed reaction mechanism on Pt(1 1 1). The hydrogenation mechanism on Pt(1 1 1) is believed to proceed first through the hydrogenation of ethylene to surface-bound ethyl (CH_3CH_2–) groups; the ethyl species has been shown to undergo facile H–D exchange before the second hydrogen is added and ethane desorbs [39]. Both the exchange and hydrogenation reactions are limited by the formation of ethyl groups [39]. It is thus likely that a similar reaction mechanism occurs on the Co, Pd, and bimetallic supported particles. Note that it would not be possible to draw this conclusion from the investigation of C_2D_4 hydrogenation with D_2.

The hydrogenation of fully deuterated ethylene (C_2D_4) with pre-adsorbed D_2 was also investigated on the mono- and bimetallic particles. Fig. 4b shows the detected mass to charge ratio during the TPD normalized to the overall signal from $m/z = 31$. In this case as well, making a comparison of amounts is difficult due to cracking patterns and isomers. Most likely there is some adsorbed H on the particles from the background, as indicated by the detection of $m/z = 35$ and 33. In the case of D_2 reaction with C_2D_4 (Fig. 4b), the relative fraction of C_2D_6 ($m/z = 36$) is higher than in the case of D_2 reaction with C_2H_4 ($m/z = 32$, Fig. 4a), suggesting that self-hydrogenation occurs in parallel with hydrogenation from the pre-adsorbed D_2.

Fig. 5 shows temperature programmed reaction spectra (TPRS) of C_2D_4 with pre-adsorbed D_2 on various surfaces. The desorption of ethylene (de-

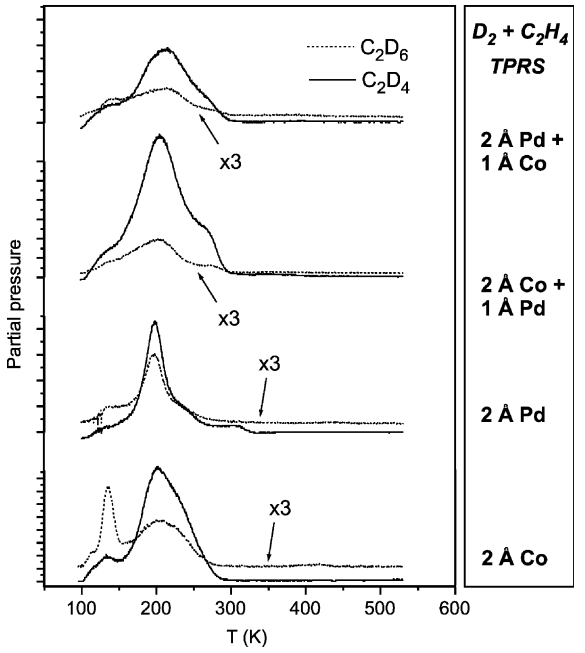

Fig. 5. Temperature programmed reaction spectra of C_2D_4 after a pre-dose of D_2; the sample was exposed to both gases at 100 K.

tected as $m/z = 32$) from the π-bonded configuration is detected at approximately 130 and 200 K for the Co, Pd, and the bimetallic particles. Desorption of ethylene from the di-σ bonded configuration is clearly observed at 265 K for the bimetallic particles, but not so much from the pure Pd or Co particles. For Pd, it has been shown that the adsorption of H_2 shifts some di-σ bonded ethylene to the π-bonded state [18,38]. On the pure Co particles, fully deuterated ethane (C_2D_6) evolves at 130 and 200 K, suggesting that the hydrogenation reaction occurred from the π-bonded ethylene and the pre-adsorbed deuterium. These reaction temperatures correspond with the two desorption temperatures of π-bonded ethylene from the Co particles and not with the desorption temperatures of hydrogen. Pi-bonded ethylene is regarded in the literature as the precursor to ethylene hydrogenation [16,40]. On the pure Pd particles, though there is also desorption of ethylene from the π-bonded state near 130 K, the hydrogenation of ethylene mainly takes place concurrent with the desorption of ethylene from the π-bonded state at 200 K. If the hydrogenation reaction takes place with sub-surface hydrogen coming to the surface at 200 K on the Pd particles [38], the reaction could only take place at 200 K, and not concurrent with the lower-desorption state of ethylene. Alternatively, it is possible that only the more strongly bound π-bonded state is a precursor to ethylene hydrogenation, or thirdly that the higher temperature is required for mobility of one of the precursors on the Pd particles. In any case, the single possible temperature for hydrogenation on the Pd particles contrasts the two possible hydrogenation temperatures on the Co particles.

On the bimetallic particles, the overall amount of ethylene hydrogenation is slightly less than on the pure Co or Pd particles (Fig. 5). When 1 Å Pd is covering 2 Å Co particles, there is a small amount of hydrogenation near 130 K, presumably due to the Co underneath, but the majority of hydrogenation occurs near 200 K, as it does on the pure Pd particles. When 1 Å Co is covering 2 Å Pd, there is more hydrogenation at 130 K than when Co forms the core rather than the shell.

In contrast to the unoxidized particles, no reaction was observed on the oxidized Co-containing particles when D_2 was pre-dosed before an ethylene TPD. Only a small trace of hydrogenation was observed on the Pd particles, presumably because a small amount of hydrogen was present (see Fig. 2b). On the oxidized Co-containing particles, hydrogen adsorption is inhibited (Fig. 2b), thus also inhibiting hydrogenation. In short, the oxidized Co-containing particles are unreactive—even when there is a partial Pd shell on top of them, or a Pd core underneath a partial Co shell.

We were not able to detect any residual carbon after CO-TPD measurements, suggesting there was no appreciable dissociation of CO. Likewise, we were not able to detect any reaction of H_2 and CO to CH_4, H_2O, CH_3OH, or CO_2 on the bimetallic particles during sequential and simultaneous dosing at 100 K and heating to 530 K in ultra-high vacuum.

4. Conclusions

The reactive properties of pristine and oxygen-covered bimetallic Co–Pd particles have been

investigated using TPD and TPRS. Hydrogen and CO adsorption is facile on the non-oxidized particles, but is severely inhibited on the oxidized bimetallic and pure Co particles; Pd particles become covered with a chemisorbed oxygen overlayer which still allows a small amount of H_2 adsorption. This suggests that oxidized Co or Co–Pd particles should be less active than unoxidized ones in the Fischer–Tropsch conversion of $CO + H_2$ to higher hydrocarbons because CO and H_2 cannot adsorb. The interaction of ethylene with the bimetallic Co–Pd particles is similar to the interaction of ethylene with Pd or Co particles, where it is π-bonded below 230 K and di-σ bonded from $\sim$230 to 270 K. At 270 K it begins to desorb or decompose to form ethylidyne, liberating hydrogen. In contrast, on the oxidized Co-containing particles, ethylene is only able to adsorb in the π-bonded state and formation of the di-σ bonded state, and thus also the formation of ethylidyne, is inhibited. To slightly different degrees, the bimetallic or monometallic particles are active for ethylene hydrogenation; the oxidized particles are essentially non-active for ethylene hydrogenation. These reactive studies indicate that the reduction of CoO to the metal could be of prime importance for the Fischer–Tropsch reaction.

Acknowledgements

Support for this work was provided by the Max-Planck Society and the Deutsche Forschungsgemeinschaft. A.C. thanks the Humboldt Foundation for a fellowship. We also wish to thank J. Abad for help with some of the measurements and Dr. Thomas Risse (FHI) for valuable discussions.

References

[1] F. Fischer, H. Tropsch, Brennstoff-Chem. 7 (1926) 97.
[2] F. Fischer, K. Meyer, Brennstoff-Chem. 12 (1931) 225.
[3] H. Pichler, H. Buffleb, Brennstoff-Chem. 21 (1940) 273.
[4] H. Schulz, Appl. Catal. A: Gen. 186 (1999) 3.
[5] H. Pichler, in: W. Frankenburg, E. Rideal, V. Komarewsky (Eds.), Advances in Catalysis, vol. IV, Academic Press, New York, 1952, p. 271.
[6] B.H. Davis, Fuel Process. Technol. 71 (2001) 157.
[7] L. Guczi, L. Borko, Catal. Today 64 (2001) 91.
[8] L. Guczi, L. Borko, Z. Schay, D. Bazin, F. Mizukami, Catal. Today 65 (2001) 51.
[9] N. Tsubaki, S. Sun, K. Fujimoto, J. Catal. 199 (2001) 236.
[10] L. Guczi, Z. Schay, G. Stefler, F. Mizukami, J. Mol. Catal. A 141 (1999) 177.
[11] H. Idriss, C. Diagne, J.P. Hindermann, A. Kinnemann, M.A. Barteau, Proceedings, 10th International Congress on Catalysis, Budapest, 1992;
L. Guczi, F. Solymosi, P. Tetenyi (Eds.), vol. C, Elsevier, Budapest, 1992, p. 2119.
[12] M.P. Kapoor, A.L. Lapidus, A.Y. Krylova, Proceedings, 10th International Congress on Catalysis, Budapest, 1992;
L. Guczi, F. Solymosi, P. Tetenyi (Eds.), vol. C, Elsevier, Budapest, 1992, 2119.
[13] W. Jusczyk, Z. Karpinski, D. Lomot, J. Pielaszek, Z. Paal, A.Y. Stakheev, J. Catal. 142 (1993) 617.
[14] F.B. Noronha, M. Schmal, C. Nicot, B. Moraweck, R. Frety, J. Catal. 168 (1997) 42.
[15] S. Bischoff, A. Weight, K. Fujimoto, B. Lücke, J. Mol. Catal. A 95 (1995) 259.
[16] N. Sheppard, C.D.L. Cruz, Adv. Catal. 41 (1996) 1.
[17] N. Sheppard, C.D.L. Cruz, Adv. Catal. 42 (1998) 181.
[18] M. Frank, M. Bäumer, R. Kühnemuth, H.-J. Freund, J. Vac. Sci. Technol. A 19 (2001) 1497.
[19] M.E. Bridge, R.M. Lambert, Surf. Sci. 82 (1979) 413.
[20] G.R. Castro, J. Küppers, Surf. Sci. 123 (1982) 456.
[21] M. Gierer, H. Over, P. Rech, E. Schwarz, K. Christmann, Surf. Sci. 380 (1997) L201.
[22] T. Hill, M. Mozaffari-Afshar, J. Schmidt, T. Risse, S. Stempel, M. Heemeier, H.-J. Freund, Chem. Phys. Lett. 292 (1998) 524.
[23] G.W. Simmons, Y.-N. Wang, J. Marcos, K. Klier, J. Phys. Chem. 95 (1991) 4522.
[24] E. Shimada, H. Yamashita, S. Matsumoto, Y. Ikuma, H. Ichimura, J. Mater. Sci. 34 (1999) 4011.
[25] E.H. Voogt, A.J.M. Mens, O.L.J. Gijzeman, J. Geus, Surf. Sci. 373 (1997) 210.
[26] F.P. Leisenberger, G. Koller, M. Sock, S. Surnev, M.G. Ramsey, F.P. Netzer, B. Klotzer, K. Hayek, Surf. Sci. 445 (2000) 380.
[27] G. Zheng, E.I. Altman, Surf. Sci. 462 (2000) 151.
[28] A. Steltenpohl, N. Memmel, Surf. Sci. 443 (1999) 13.
[29] M. Frank, M. Bäumer, Phys. Chem. Chem. Phys. 2 (2000) 3723.
[30] M. Bäumer, H.-J. Freund, Prog. Surf. Sci. 61 (1999) 127–198.
[31] A.F. Carlsson, M. Naschitzki, M. Bäumer, H.-J. Freund, J. Phys. Chem. B 107 (2003) 778.
[32] R.M. Jaeger, H. Kuhlenbeck, H.-J. Freund, M. Wuttig, W. Hoffmann, R. Franchy, H. Ibach, Surf. Sci. 259 (1991) 235.
[33] K.H. Hansen, T. Worren, S. Stempel, E. Laegsgaard, M. Bäumer, H.-J. Freund, F. Besenbacher, I. Stensgaard, Phys. Rev. Lett. 83 (1999) 4120.

[34] M. Bäumer, M. Frank, M. Heemeier, R. Kühnemuth, S. Stempel, H.-J. Freund, Surf. Sci. 454 (2000) 957.
[35] S. Stempel, Doctoral Dissertation, Freie Universität, Berlin, 1998.
[36] H.-J. Freund, Faraday Discuss. 114 (1999) 1.
[37] K. Christmann, Prog. Surf. Sci. 48 (1995) 15.
[38] S. Shaikhutdinov, M. Heemeier, M. Bäumer, T. Lear, D. Lennon, R.J. Oldman, S.D. Jackson, H.-J. Freund, J. Catal. 200 (2001) 330.
[39] F. Zaera, Langmuir 12 (1996) 88.
[40] P.S. Cremer, G.A. Somorjai, J. Chem. Faraday Trans. 91 (1995) 3671.